Advances in Physics Theories and Applications
ISSN 2224-719X (Paper) ISSN 2225-0638 (Online)
Vol.16, 2013

Dielectric Function in Highly doped GaN Semiconductor

F. M. Abou El-Ela, A. Z. Mohamed
Department of Physics, Faculty of Girls,
Ain Shams University, Heliopolis, Cairo, Egypt
E-mail: fadlaeg@yahoo.com

Abstract : Inverse of Dielectric Function of highly doped GaN has been calculated by using Lindhard formalism. For simplicity collisional damping, nonparabolicity and the coupling between various electrons and holes were neglected. The inverse of the dielectric function for both Fermi- Dirac and Maxwell Boltzman distribution showed antiscreening peak at small phonon wave vector. On the contrary, both Thomas Fermi and Debye inverse of dielectric function showed screening as expected at same phonon wave vector. There is a sharp growth in the antiscreening peak in the inverse of dielectric function at carrier temperature 77 K and 300K, accompanied with a singularity at carrier concentration greater than $5x10^{24} m^{-3}$.

Key words: dielectric function, GaN and screened optical phonon scattering rate

1. Introduction

In the early 1970s, interest in GaN-based devices has risen rapidly (Nakamura et al. 1995, 1994; Mohammed and Morkoc 1996; Gelmont et al. 1993; O'Leary et al. 2006). There has been considerable interest in GaN due to its wide band gap and favorable material properties, such as high electron mobility and very high thermal conductivity. The large band gap energy of the III-nitrides insures that the breakdown electric field strength of these materials is much larger than that of GaAs (You and Ong 2000; Adachi 1994; Fawcett et al.1970).

Early studies of electron transport in polar materials neglected screening of the electron-polar interaction by free carries. At moderate and high carrier densities, however, it is important to include not only screening of this interaction, but also electron-electron interaction and scattering by ionized impurities. Ehrenreich (Ehrenreich 1959) investigated screening of the electron polar optical phonon mode interaction. Although he went so far as to treat the dynamical aspect of screening, eventually he describes the interaction in terms of static screening later. The influence of screening on carrier mobility was studied, in a series of paper (Doniach 1959; Ravish et al. 1970, 1971) on the theory of transport. There was a further step towards using the dynamic screening potential rather than static one on the inter carrier interaction potential (Meyer and Bartoli 1983; Ridley 1985; Abou El-Ela 1986, 1988; Lugli and Ferry 1983; Lugli 1985). The treatment of electron collision with plasmon-phonon coupled mode has grown in importance for plasma frequency exceeding the phonon frequency (Lugli and Ferry 1983; Lugli 1985) in view of the widespread interest in high carrier concentrations.

For carrier densities of $2x10^{24} m^{-3}$ and above in GaN screening becomes of considerable importance and its dynamics nature must be taken into account. The dielectric function $k(\mathbf{q},\omega)$ is considered as one of the most interesting factors in the investigation of electron interaction with optical phonon mode including dynamic screening behavior in semiconductor,

The Lindhard formalism **(** Lindhard 1954; Ridley 1988; Ziman 1972) is a very good approximation to the dielectric function in the weak coupling limit. It correctly predicts a number of properties of the electron gas such as screening and plasmon dispersion. This approach is commonly called the self-consistent field approximation (SCF), in which we assume that the electron respond to the total potential $v(\mathbf{q},\omega)$ and try to determine this function self-consistently.

2. The Dielectric Function in Highly Doped Semiconductor

The Lindhard formula for the dielectric constant is

$$k(\mathbf{q},\omega) = k_{\infty}(\mathbf{q},\omega)\left[1 + \frac{e^2}{\varepsilon_{\infty}\mathbf{q}^2 v}\sum_{\mathbf{k}} f_o(E_{\mathbf{k}})\left(\frac{1}{E_{\mathbf{k}-\mathbf{q}} - E_{\mathbf{k}} + \hbar\omega + i\hbar\alpha} + \frac{1}{E_{\mathbf{k}+\mathbf{q}} - E_{\mathbf{k}} - \hbar\omega - i\hbar\alpha}\right)\right] \quad (1)$$

$k_\infty(\mathbf{q},\omega)$ is the high-frequency dielectric contribution from the valence band electrons, ε_o is the permittivity of free space and ε_∞ is the corresponding permittivity. The summation in Eq. (1) is over all electron states in the conduction band weighted by the distribution function $f_o(E_\mathbf{k})$, the crystal volume is denoted by v, e is the electronic charge and $E_\mathbf{k}$ is the electron energy at wave vector k. The formula is evaluated in the usual manner with α approaching zero (collisional damping is neglected). Also, for simplicity nonparabolcity and the coupling between various electron and hole bands has been neglected, since these effects give a correction of second order. Then, one obtains

$$S = \frac{V}{2\pi^2}\int_{-1}^{1}\int_{0}^{\infty} f_o(E_\mathbf{k})\left(\frac{1}{\frac{\hbar^2\mathbf{q}^2}{2m^*}-\frac{\hbar^2\mathbf{kq}}{m^*}\cos\theta+\hbar\omega+i\hbar\alpha}+\frac{1}{\frac{\hbar^2\mathbf{q}^2}{2m^*}+\frac{\hbar^2\mathbf{kq}}{m^*}\cos\theta-\hbar\omega-i\hbar\alpha}\right)\mathbf{k}^2 d\mathbf{k}\, d(\cos\theta) \tag{2}$$

This could be rewritten as

$$S = \frac{V}{2\pi^2}\int_{0}^{\infty}\frac{m^*k}{\hbar^2\mathbf{q}} f_o(E_\mathbf{k})\ln\left(\frac{1+\frac{\mathbf{q}}{2\mathbf{k}}+\frac{m^*}{\hbar^2\mathbf{kq}}(\hbar\omega+i\hbar\alpha)}{1-\frac{\mathbf{q}}{2\mathbf{k}}-\frac{m^*}{\hbar^2\mathbf{kq}}(\hbar\omega+i\hbar\alpha)}\right)dk + \int_{0}^{\infty}\frac{m^*k}{\hbar^2\mathbf{q}} f_o(E_\mathbf{k})\ln\left(\frac{1+\frac{\mathbf{q}}{2\mathbf{k}}-\frac{m^*}{\hbar^2\mathbf{kq}}(\hbar\omega+i\hbar\alpha)}{1-\frac{\mathbf{q}}{2\mathbf{k}}+\frac{m^*}{\hbar^2\mathbf{kq}}(\hbar\omega+i\hbar\alpha)}\right)dk \tag{3}$$

Then we rewrite Eq. (1) as

$$k(\mathbf{q},\omega) = k_\infty(\mathbf{q},\omega)\left[1+\frac{e^2}{\varepsilon_\infty\mathbf{q}^2}\frac{1}{2\pi^2}\frac{m^*}{\hbar^2\mathbf{q}}\int_{0}^{\infty}\mathbf{k}\, f_o(E_\mathbf{k})\ln\left(\frac{(1+\frac{\mathbf{q}}{2\mathbf{k}})^2+(\frac{m^*}{\hbar^2\mathbf{kq}})^2(\hbar\omega+i\hbar\alpha)^2}{(1-\frac{\mathbf{q}}{2\mathbf{k}})^2-(\frac{m^*}{\hbar^2\mathbf{kq}})^2(\hbar\omega+i\hbar\alpha)^2}\right)dk\right] \tag{4}$$

A system of electrons under degenerate conditions can be studied assuming Fermi-Dirac statistics for the energy distribution in Eq. (4). For non-degenerate conditions the energy distribution takes a Maxwellian form and $k(\mathbf{q},\omega)$ can be written as

$$k(\mathbf{q},\omega) = k_R(\mathbf{q},\omega) + i\,k_I(\mathbf{q},\omega) \tag{5}$$

Where $k_R(\mathbf{q},\omega)$ and $k_I(\mathbf{q},\omega)$ are the real and the imaginary part of dielectric function respectively

2.1 Calculation the Real Part of Dielectric Function

In order to calculate the real part $k_R(\mathbf{q},\omega)$ of the dielectric function, using Fermi-Dirac and Maxwellian form of the distribution, we introduce the dimensionless variables for the simplicity:

$$\gamma = \frac{\omega_p}{\omega} \qquad \omega_p = \left(\frac{N e^2}{\varepsilon_\infty m^*}\right)^{1/2} \qquad \theta = \frac{\hbar\omega}{k_B T_e}$$

$$y = \frac{k}{k_o} \qquad x = \frac{q}{k_o} \qquad k_o = \left(\frac{2m^*\omega}{\hbar}\right)^{1/2} \tag{6}$$

$$\Delta_f = \frac{E_f}{\hbar\omega} \qquad \Delta_o = \frac{E_{fo}}{\hbar\omega} \qquad E_{fo} = \frac{\hbar^2}{2m^*}(3\pi^2 N)^{2/3}$$

The inverse of dielectric function depends on both the wave vector $\mathbf{q}$ and the frequency of the phonon ω_q. For simplicity, we assume that ω_q equals the longitudinal phonon frequency ω. E_{fo} and E_f Define as Fermi energy at T =0 and T_e respectively at carrier concentration N where T_e is the electron temperature.

The Fermi-Dirac distribution becomes

$$f_o(E_{\mathbf{k}}) = [1 + \exp[\theta\,(y^2 - \Delta_f)]]^{-1} \tag{7}$$

While the Maxwellian-Boltzmann distribution takes the form

$$f_o(E_{\mathbf{k}}) = \exp[-\theta\,(y^2 - \Delta_f)] \tag{8}$$

The real part $k_R(\mathbf{q},\omega)$ for Fermi-Dirac distribution is obtained as

$$\frac{k_R(\mathbf{q},\omega)}{k_\infty(\mathbf{q},\omega)} = 1 + \frac{3}{8}\frac{\gamma^2}{\Delta_o^{3/2}}\frac{1}{x^3}\int_0^\infty y\frac{1}{1+\exp\left[\theta\,(y^2-\Delta_f)\right]}\ln\left[\frac{(1+\frac{x}{2y})^2 - \frac{1}{4x^2y^2}}{(1-\frac{x}{2y})^2 - \frac{1}{4x^2y^2}}\right]dy \tag{9}$$

The real part $k_R(\mathbf{q},\omega)$ for the Maxwellian form is derived using Eqs. (4), and (8) and one obtains

$$\frac{k_R(\mathbf{q},\omega)}{k_\infty(\mathbf{q},\omega)} = 1 + \frac{e^2 m^*}{2\pi^2\varepsilon_\infty\hbar^2}\frac{1}{\mathbf{k}_o}\frac{1}{x^3}\int_0^\infty y\,\exp\left[-\theta(y^2-\Delta_f)\right]\ln\left[\frac{(1+\frac{x}{2y})^2 - \frac{1}{4x^2y^2}}{(1-\frac{x}{2y})^2 - \frac{1}{4x^2y^2}}\right]dy \tag{10}$$

In order to avoid the singularities in the integral function (10) we divided these integral into the following intervals

1- from 0 to $\frac{1}{2}\left|x-\frac{1}{x}\right|$ 2- from $\frac{1}{2}\left|x-\frac{1}{x}\right|$ to $\frac{1}{2}\left|x+\frac{1}{x}\right|$ 3- from $\frac{1}{2}\left|x+\frac{1}{x}\right|$ to ∞

Static Dielectric Function

The static screening function is obtained with $\omega\to 0$; For Fermi-Dirac distribution we use Thomas- Fermi screening length defined by

$$q_o^2 = \left(\frac{e^2}{\varepsilon_s}\right)N(E_f) \qquad N(E_f) = \frac{m^* k_f^o}{\pi^2\hbar^2}, \qquad q_o^2 = \frac{e^2 m^* k_f^o}{\varepsilon_s\pi^2\hbar^2} \quad \text{and}$$

$$\frac{k(q,0)}{k_\infty(q,0)} = \left[1 + \frac{q_o^2}{q^2}\right] = \left[1 + \frac{3}{4}\left(\frac{y}{x}\right)^2\frac{1}{\Delta_o}\right] \tag{11}$$

For Maxwellian distribution, on the other hand, we use Debye screening length define as

$$q_o^2 = \frac{e^2 N}{\varepsilon_s k_B T_e}$$

To obtain Debye screening we put $E_{fo} = \frac{3}{2} k_B T_e$ in Thomas- Fermi

$$\frac{k(q,0)}{k_\infty(q,0)} = \left[1 + \frac{q_o^2}{q^2}\right] = \left[1 + \frac{3}{4}\left(\frac{y}{x}\right)^2 \frac{\hbar\omega}{E_{fo}}\right] = \left[1 + \frac{1}{2}\left(\frac{y}{x}\right)^2 \theta\right] \tag{12}$$

2.2 Calculation the Imaginary Part of Dielectric Function

$$\frac{k_I(\mathbf{q},\omega)}{k_\infty(\mathbf{q},\omega)} = \frac{e^2 m^{*2} k_B T_e}{2\pi\varepsilon_\infty \hbar^4 q^3} \ln \left[\frac{1 + \exp\left(\frac{-m^*}{2\hbar^2 \mathbf{q}^2 k_B T_e}\left(\frac{\hbar^2\mathbf{q}^2}{2m^*} - \hbar\omega\right)^2 + \frac{E_f}{k_B T_e}\right)}{1 + \exp\left(\frac{-m^*}{2\hbar^2 \mathbf{q}^2 k_B T_e}\left(\frac{\hbar^2\mathbf{q}^2}{2m^*} + \hbar\omega\right)^2 + \frac{E_f}{k_B T_e}\right)}\right] \tag{13}$$

which may be rewritten after using dimensionless parameter, as

$$\frac{k_I(\mathbf{q},\omega)}{k_\infty(\mathbf{q},\omega)} = \frac{3\pi^2}{16} \frac{\gamma^2}{\Delta_o^{3/2}} \frac{1}{x^3} \ln \left[\frac{1 + \exp\left(\theta\left(\Delta_f - \frac{(x - \frac{1}{x})^2}{4}\right)\right)}{1 + \exp\left(\theta\left(\Delta_f - \frac{(x + \frac{1}{x})^2}{4}\right)\right)}\right] \tag{14}$$

3.Results and discussion

We have studied the real and imaginary parts of the dielectric function, which were derived in previous section. This function depends on both the wave vector $\mathbf{q}$ and the frequency of the phonon ω_q. For simplicity, we assumed that ω_q equals the longitudinal phonon frequency ω.

Both real and imaginary parts are strong functions of carrier concentration N and electron temperature T_e through their dependence on Fermi energy. Table (1) summarizes the variation of $\frac{E_f}{\hbar\omega}$ with both N and T_e. Our GaN used parameters are taken from O'Leary et al.(2006), which were originally reported by Foutz et al.(1999) and Lambrecht and Segall (1994).

Inverse of real part of dielectric function ($\frac{k_\infty(\mathbf{q},\omega)}{k_R(\mathbf{q},\omega)}$) versus normalized phonon wave vector (X) for various electron concentrations of $0.5\text{x}10^{24}$, $2.5\text{x}10^{24}$, $5\text{x}10^{24}$ and $7.5\text{x}10^{24}$ m^{-3} at electron temperature 300K and 77K were presented in Figs. (1- a-d) and Figs. (2- a-d) respectively; where k_o is defined as electron wave vector corresponding optical phonon energy $\hbar\omega$. In each graph we present the variation due to Fermi-Dirac distribution, Maxwell Boltzmann distribution and static dielectric function by using both Thomas Fermi and Debye screening. For small phonon wave vector the ω_q is actually greater than ω and the real part of inverse Lindhard dielectric

function is greater than one as could be seen in the Figs. (1- a-d) with both Fermi-Dirac and Maxwell Boltzmann distributions; In other words, the interaction potential is enhanced. This is commonly known as the antiscreening effect (Meyer and Bartoli 1983; Ridley 1985; Abou El-Ela 1986; Ridley 1988) which occurs when the phase velocity of the phonon is larger than the thermal velocity of the electron. In such a situation, the free electrons cannot be adjusted rapidly enough to screen lattice potential; therefore, the build-up of charge results in the enhancement of the lattice potential. On the other hand, for large phonon wave vector the phonons have a comparable or smaller phase velocity than the thermal velocity of the electron; so that, these phonons are screened by the free carriers, leading to the normal response to the electron motion.

The following point can be concluded from the graphs (1- a-d) and (2- a-d}
1- The real part of inverse Lindhard dielectric function for both Fermi-Dirac and Maxwell distributions showed antiscreening at small X while both Thomas Fermi and Debye real part of inverse Lindhard dielectric function showed screening as expected at the corresponding X .
2- At electron temperature 300K and carrier concentrations less than $2.5x10^{24}$ m^{-3}, both Fermi-Dirac and Maxwell Boltzmann distribution function have similar influence on the variation of real part of inverse Lindhard dielectric function with X , but this is not same for electron temperature 77K.
3- There is a sharp growth in the antiscreening peak in the real part of inverse Lindhard dielectric function at both carrier temperatures 77K and 300K, accompanied with a singularity at carrier concentration more than $5x10^{24}$ m^{-3}.
4- Taking account of the imaginary part of the dielectric function is important to avoid singularity.

The Inverse of Lindhard dielectric function variation at lattice temperature300K of the real and total part is shown in Figs. (3-a,b) with carrier concentrations $0.5x10^{24}$ m^{-3} and $2.25x10^{24}$ m^{-3} respectively. The behavior shown in Fig.(3-a), is determined by the real part, since imaginary part is only important at carrier concentration above $1x10^{24}$ m^{-3}; the influence of the imaginary part is to prevent $\left[k_R^2(\mathbf{q},\omega)+k_I^2(\mathbf{q},\omega)\right]^{-1}$ from diverging as is shown in Fig. (3-b).
Figs. (4-a,b) represent Inverse of total Lindhard dielectric function at lattice temperature 300K for various carrier concentration, and for several values of electron temperature.
The inverse of total Lindhard dielectric function value increases with increasing carrier concentration, while cooling the electron temperature also increases the value of antiscreening peak. In addition, the position of this peak was shifted to higher normalized phonon wave vector. The inverse of total Lindhard dielectric function value can be divided into three regions according to normalized phonon wave vector value (X)
a- For $0.7 \geq X$, behaved as antiscreening and has a value larger than 1.
b- For $0.7 \leq X \leq 1.0$, behaved as screening and has a value smaller than 1. This behavior appears very strongly only at high electron temperature or high carrier concentration.
c- For $X \geq 1$, the motion of the free electron does not affect the phonon vibrations and has a value approximately equals 1

4. Conclusion

In present work, we have investigated the inverse of dielectric function in bulk GaN by applying the Lindhard formalism. For simplicity nonparabolicity, collisional damping and the coupling between various electrons and holes have been neglected. The main emphasis of inverse dielectric function for both Fermi- Dirac and Maxwell Boltzman distribution showed antscreening peak at small phonon wave vector. At electron temperature 300K and carrier concentrations less than $2.5x10^{24}$ m^{-3}, both Fermi-Dirac and Maxwell Boltzmann distribution function have similar influence on the variation of the inverse dielectric function with phonon wave vector, but this is not so for electron temperature 77K. Taking account of the imaginary part of the dielectric function is important to avoid the singularity. The principle purpose of this study is to show how the various parameters such as, carrier concentrations and electron temperature could change the shape of dielectric function; consequently it become easier to understand the influence of dielectric function on scattering rate of polar optical phonon mode.

5. References:

Abou El-Ela F., Riddoch, F.A, Davis, M. , and Ridley, B.K, Proc. Int. Conf. Semiconductor physics, Stockholm,

P.1567(1986).
Abou El-Ela, F. and B.K. Ridley, B.K. "Hot carriers in semiconductor", USA, Solid State Electronics, Vol. 314, P. 691(1988).
Adachi, S., " GaAs and Related Materials, Bulk semiconducting and Superlattice Properties", World Scientific, Singapore, (1994).
Doniach, S. , Proc. Phys. Soc., London, 73, 849 (1959).
Ehrenreich, H. , J. Phys. Chem. Solids, 8, 130 (1959).
Foutz, B. E. , O'Leary, S.K. , Shur , M.S. and Eastman, L.F. , J. Appl. Phys. 85 7727 (1999).
Fawcett, W., Boardman , A. D. and Swain, S. , J. Phys. Chem. Solids 31 1963 (1970).
Gelmont, B., Kim, K. and Shur, M. , J. Appl. Phys. 74 (3) 1818 (1993).
Lindhard , J., Dan. Vidensk. Selsk. Mat.- Fys. Medd.**,** 28, 8 (1954)**.**
Lugli, P. and Ferry, D. K. , Physica B , 117, 251 (1983).
Lugli , P., "Electron- Electron Effect in semiconductor", Ph.D. Thesis, Colarda State University, USA (1985).
Lambrecht , W. R .L. and Segall, B., " Properties of Group III Nitrides", EMIS Data reviews Series, ed. By J. H. Edgar (Inspec , London) Chap. 4 (1994).
Mohammed, S. N. and Morkoc, H., Prog. Quantum Electron. 20 361 (1996).
Meyer , J .R. and Bartoli, F. J. , Phys. Rev., B28, 915,(1983).
Nakamura, S., Mukai,T. and Senoh, M., *Appl. Phys. Lett*. 64 1687 (1994).
Nakamura, S., Senoh, M., Iwasa, N. , Nagahama, S., and Mukai, T., Jpn. I. Appl. Phys., Part 2 34 L1332 (1995).
O'Leary, S.K., Foutz, B.E., Shur , M.S. and Eastman, L.F. , J. Mater Sci: Mater Electron 17 87 (2006).
Ravich, Yu.I. and Morgovskii, L.Ya., Sov. Phys. Semicond., 3, 1278 (1970).
Ravich, Yu.I. , Efimova, B.A. and Tamarchenko, V.I. , Phys. Status. Solidi, B43, 11 (1971).
Ridley,B.K., Adv. Solid State Phys.(Festkorperprobleme), 25 449 (1985).
Ridley ,B.K. , " Quantum Processes in Semiconductors ", Claredon Press, Oxford (1988).
You, A .H. and Ong, D.S. , Proc. ICSE 2000., 182(2000).
Ziman , J.M.,"The Principle of Theory of Solids", Cambridge university press, Cambridge (1972).

Table (1) the variation of Δ_f with both N and T_e in GaN

N $(1x10^{24}\,m^{-3})$	γ	Δ_o	Δ_f 300K	Δ_f 77K
0.5	0.2825	0.1247	-0.4095	0.07914
2.0	0.5651	0.3144	0.049105	0.3015
2.5	0.6318	0.3648	0.13389	0.3499
5.0	0.8935	0.5791	0.436	0.5869
7.5	1.094	0.7588	0.6536	0.7361

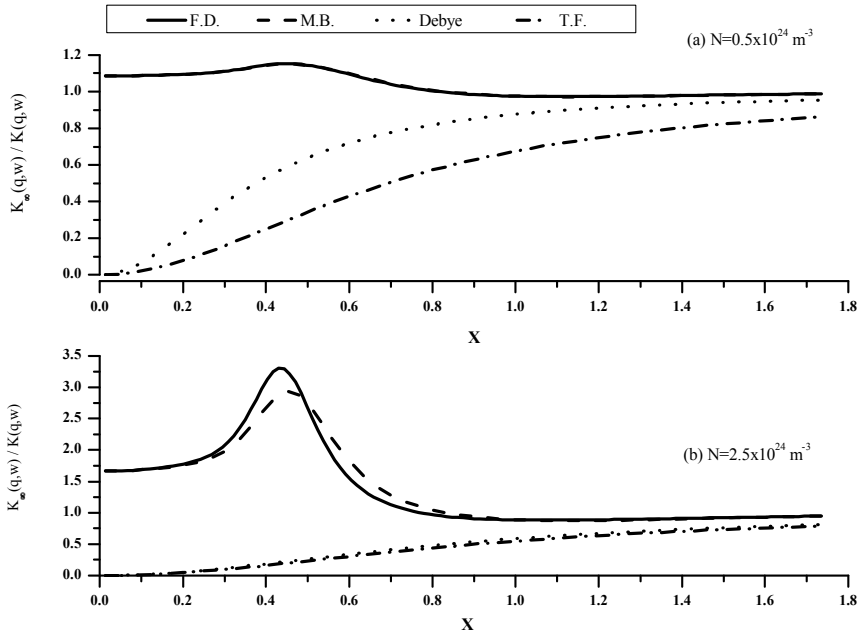

Figs. (1-a,b) the real part of inverse Lindhard dielectric function at lattice temperature 300K for various distribution function for electron concentrations $0.5x10^{24}$ and $2.5x10^{24}$respectively.

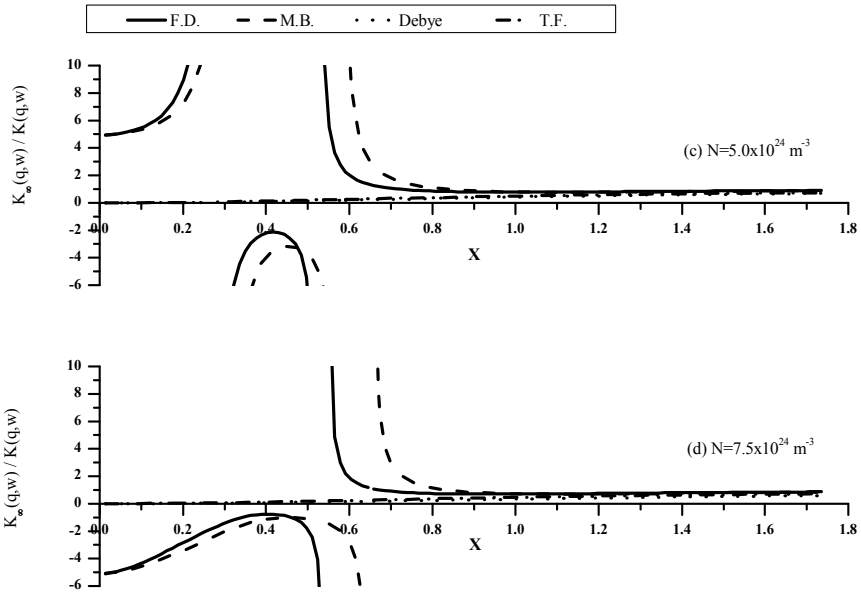

Figs. (1-c,d) the real part of inverse Lindhard dielectric function at lattice temperature 300K for various distribution function for electron concentrations $5x10^{24}$ and $7.5x10^{24}$ respectively

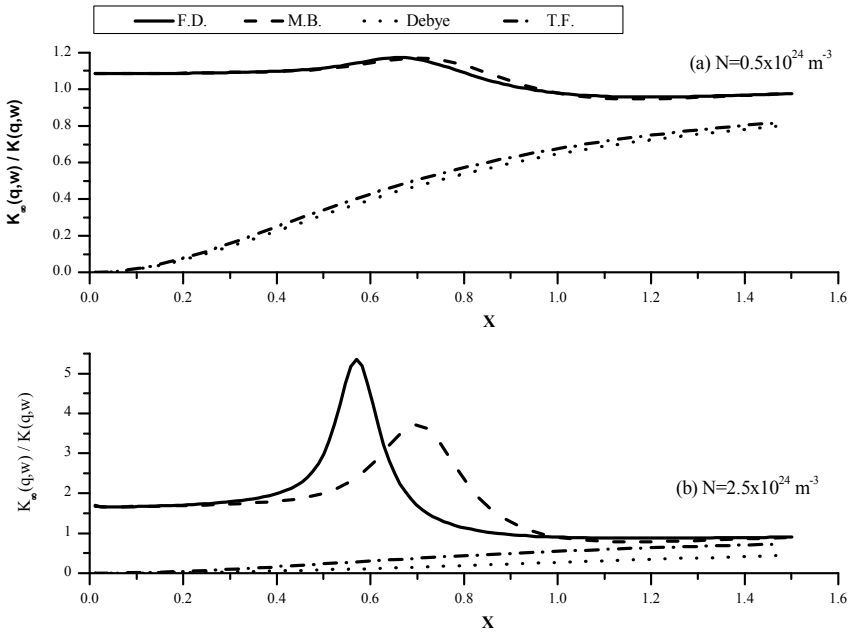

Figs. (2-a,b) the real part of inverse Lindhard dielectric function at lattice temperature 77K for various distribution function for electron concentrations $0.5x10^{24}$ and $2.5x10^{24}$respectively.

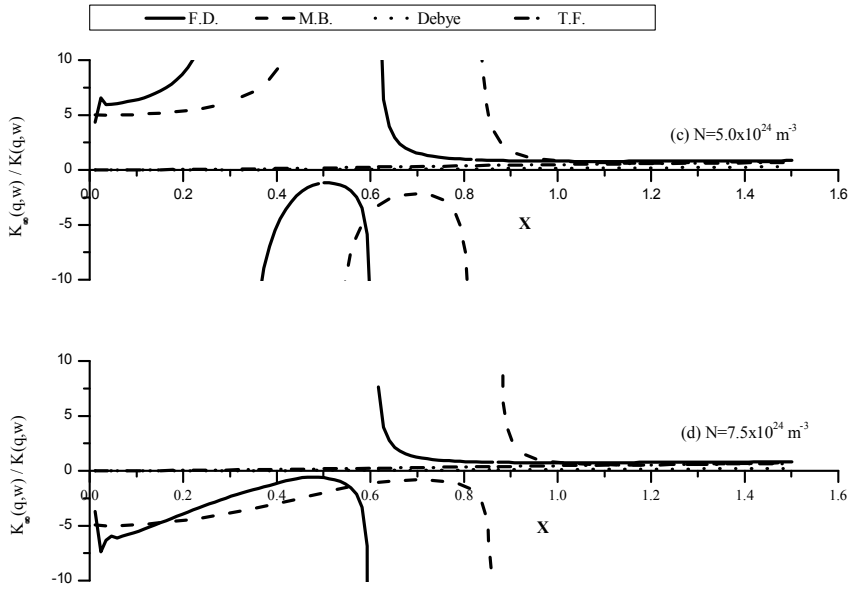

Figs. (2-c,d,) the real part of inverse Lindhard dielectric function at lattice temperature77K for various distribution function for electron concentrations $5x10^{24}$ and $7.5x10^{24}$ respectively.

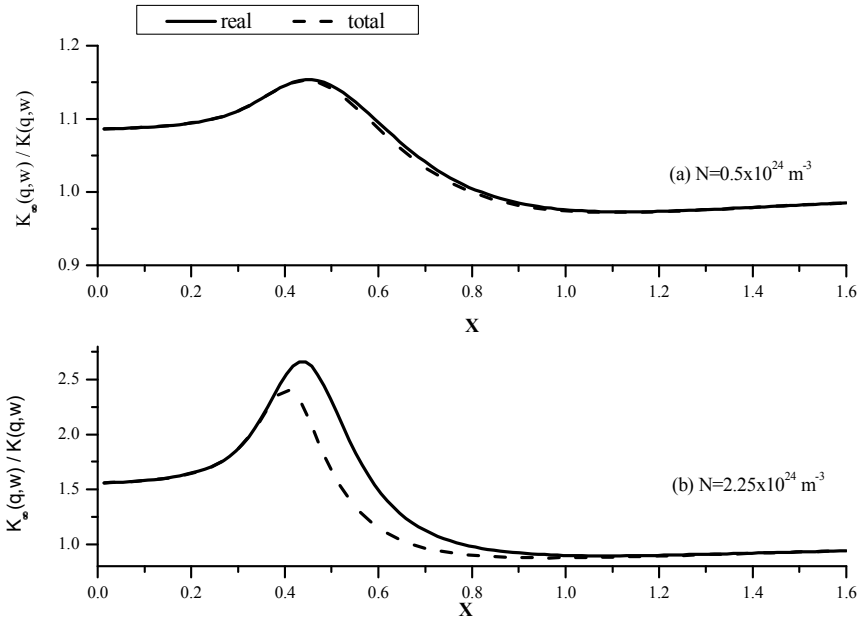

Figs. (3-a,b) Inverse of Lindhard dielectric function at lattice temperature300K showing the real and the total part with carrier concentration of 0.5x10^{24} and 2.5x10^{24}respectively

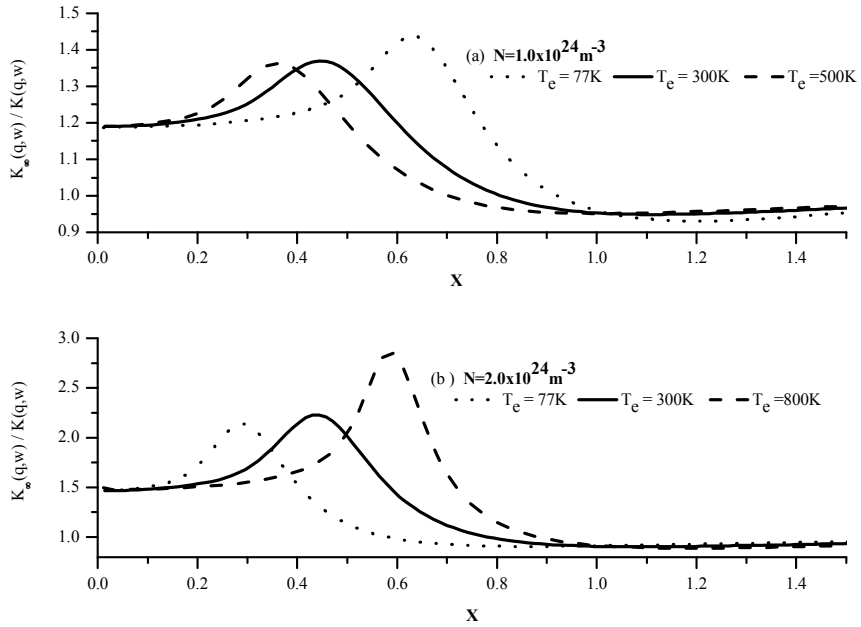

Figs.(4-a,b) Inverse of total Lindhard dielectric function at lattice temperature 300K for carrier concentration 1.0x10^{24} and 2.0 x10^{24}respectively respectively, and for several values of electron temperature.